Journal of Statistical Physics, Vol. 62, Nos. 3/4, 1991

Field-Induced Percolation in a Polarized Lattice Gas

Marc Aertsens[1] and Jan Naudts[2]

Received July 18, 1990; final October 10, 1990

We introduce a lattice gas model with particles carrying a charge either $+1$ or -1 and drifting in opposite directions due to the presence of an external field. Our numerical simulations show the formation of polarized clusters elongated along the direction of the field. At low enough temperatures the clusters percolate through the system in a similar way as in the strip phase of the driven lattice gas model. A possible application of the model can be found in microemulsions.

KEY WORDS: Driven lattice gas model; dynamic percolation, microemulsions; nonequilibrium phase diagram.

1. INTRODUCTION

Lattice gas models under far-from-equilibrium conditions are of recent interest. Two distinct situations have been studied in detail. After a quench from the high-temperature gas phase into the low-temperature solid phase one observes nucleation and growth of particle aggregates. The interesting question here is how the system evolves toward equilibrium. In another scenario, the particles are assumed to drift in a given direction due to the presence of an external field. A model system in this case is the so-called *driven lattice gas.*[1-13] A slightly different version is known as the *van Beijeren/Schulman model.*[14,15] The relevant question is now how to characterize the stationary states. In particular, for a strong drift and at sufficiently low temperatures stationary states were observed in which the low- and high-density phases are separated into a regular repetition of strips ($d=2$) or cylinders ($d=3$) aligned along the direction of the external field. From now on we will refer to this phase as the *strip phase.*

An obvious feature of the strip phase is the percolation of clusters of

[1] Limburgs Universitair Centrum, Universitaire Campus, 3610 Diepenbeek, Belgium.
[2] Departement Fysica, Universiteit Antwerpen (UIA), 2610 Antwerpen, Belgium.

0022-4715/91/0200-0609$06.50/0

particles along the direction of the field. An apparent consequence of the anisotropy introduced by the external field is that percolation can occur at particle densities which are too low for allowing percolation in the absence of the field. Marro and Vallés[7] have observed percolation during simulations on square lattice systems at density $\rho = 0.20$, while in the absence of the external field and in the gas phase percolation can[16] only occur for $\rho \geqslant 0.50$. In $d = 3$ on a simple cubic lattice the lowest density at which percolation occurs in the gas phase is[17,18] $\rho \simeq 0.22$ at $T = 0.96 T_c$. We checked that in the presence of a strong field the strip phase exists even at a density of $\rho = 0.08$.

In the present paper we study a model which is slightly more complicated than the driven lattice gas. Instead of letting all particles drift in the same direction, we consider particles carrying charges either $+1$ or -1 and drifting in opposite directions. The reason for introducing the new model is twofold: (i) we conjecture that steric hindrance of particles all moving in the same direction is a dominant mechanism in the formation of the strip phase of the driven lattice gas; we are interested in a more gentle mechanism; for convenience we call it *polarization* of clusters of charged particles (although one could object the crippled analogy with real electric systems); (ii) from the point of view of physics, both kinds of systems are of interest; a nice experimental realization of a lattice gas with two types of charged particles is found in water-in-oil microemulsions, which are discussed below.

Water-in-oil microemulsions consist of small nanometer-sized droplets suspended in liquid oil. The water droplets are electrically conductive and can be charged positively as well as negatively. Charges larger than $\pm e$ are very unlikely at low density.[34] Application of an electric field leads to a drift of the charged droplets. They can be monitored by measuring the electric current. It was observed that a slight increase in the concentration of droplets can raise the electric conductivity by several orders of magnitude. The phenomenon was explained as a percolation transition[19-23]: a cluster of droplets connecting both electrodes carries a huge electric current because charges can easily hop from one droplet to the next. Complementary information was obtained by means of Monte Carlo simulations.[25-29]

The complicated dependence of the percolation transition on temperature, density, and electric field has given rise to much interest. Percolation thresholds as low as 0.08 volume fraction have been reported.[19,20] Several arguments have been put forward[25-27] explaining why percolation occurs at densities well below the percolation threshold of about 0.35 for percolation of randomly positioned nonoverlapping spheres in a continuum.[30] However, none of these have taken into account the effects of an external field.

Measurements at a volume fraction of about 25% of droplets show that the percolation transition depends on the field strength.[24] The anisotropy induced by the field has been confirmed by means of Kerr effect measurements.[31] Clusters of particles are elongated in the direction of the field. The nonlinear field dependence of the electric current was explained in a phenomenological way[32] by an increased mobility for a combined conduction process in which charged droplets move back and forth between slightly polarized elongated clusters. We believe that those effects can be reproduced by the model presented here. However, the present study has been limited to that part of the phase diagram where the strip phase is observed. We are not yet able to compare with experiments on microemulsions. The conditions under which the percolation transition in water-in-oil microemulsions can be studied correspond to the gas phase of the model, close to the phase separation temperature. The strip phase occurs below the phase separation temperature. Hence it is not obvious wether the percolation transition observed experimentally is related to the formation of a strip phase.

The model is introduced in Section 2. Details of the simulations are given in Section 3. The results are discussed in Section 4. Conclusions follow in Section 5. Some early results of our work have been published before.[33]

2. THE MODEL

We consider a lattice gas of particles each carrying a charge of either $+1$ or -1. The total charge of the system is zero. From a static point of view the model can be considered as a diluted Ising model. Hence we assign to every site i of a simple cubic lattice two variables: t_i and s_i. The variable t_i is 1 if the site is occupied, and zero otherwise. The variable s_i represents the charge of the particle: $s_i = \pm 1$. In the absence of an electric field the Hamiltonian of the system is the usual lattice gas Hamiltonian

$$H = -4J \sum_{|i-j|=1} t_i t_j \tag{1}$$

where $4J$ is the nearest neighbor attraction between the particles.

An electric field E is chosen parallel with the vertical z axis. The positive pole is put at $z = +\infty$. Hence, the formal Hamiltonian of the system in presence of the field reads

$$H = -4J \sum_{|i-j|=1} t_i t_j + E \sum_i t_i s_i z_i \tag{2}$$

where z_i is the z coordinate of site i. If all charges have the same nonzero

value (either $+1$ or -1), the Hamiltonian (2) is that of the driven lattice gas.

The choice of boundary conditions for the simulation of a finite system with Hamiltonian (2) poses serious problems, especially on the upper and lower edges of the system. An obvious choice consists of periodic boundary conditions in the x and y directions and fixed boundary conditions in the z direction. E.g., a layer of fixed particles at $z=0$ and $z=L$ leads to an accumulation of negative particles near the upper edge of the system, and positive particles near the lower edge. This can be prevented by turning all negative particles reaching the upper edge of the system into positive particles, and similarly at the lower edge. Simulations under these conditions reveal important disturbances of the particle distribution near the upper and lower edges. Also, other choices of boundary conditions along the z direction were found not to be acceptable.

We have opted for periodic boundary conditions also in the z direction. Strictly, this choice is not compatible with (2) as a Hamiltonian, since the latter is not periodic in z. Indeed, when a negative particle disappears at the upper edge and reappears at the lower edge of the system, its potential energy drops by the amount LE (where L is the height of the system). Nevertheless, we can use (2) formally if arithmetic in z is performed modulo L, since only local differences (gradients) of H enter into the transition rates.

Next we discuss the choice of dynamics. Two mechanism are implemented: one for particle motion and a separate one for charge exchange between neighboring particles. Both mechanisms use a coordination number of 18, the usual nearest and next nearest neighbor positions of a simple cubic lattice. Hence, while according to Hamiltonian (2) particles attract only between 6 neighboring positions, they can move to any empty site out of 18 neighboring sites. Similarly, a particle can exchange its charge with any particle on one of 18 neighboring sites. In this way we trv to avoid steric hindrance efects. In the driven lattice gas particle jumps are only allowed to 6 nearest neighbors. We expect steric hindrance to be important then. The coordination number of 18 increases the possibility of motion along the direction of the field and avoids freezing of the system due to steric hindrance.

The particles move according to Kawasaki dynamics. During one Monte Carlo step (MCS) each particle tries exactly once to move to a randomly chosen neighboring site. If the chosen site is occupied, the particle does not move. Otherwise, using (2), the change in energy is calculated and the move is accepted using the Metropolis criterion. Due to the particle–hole exchange the individual particles diffuse and the cluster configuration changes.

The algorithm for charge exchange is executed N times after each completion of the particle–hole exchange algorithm. For each particle a neighboring site is chosen randomly. If this site is empty or occupied with a particle bearing the same charge, nothing happens and one continues with the next particle. If both sites are occupied and have the same z coordinate, the charges are exchanged. Finally, if the z coordinates differ, the largest charge is placed with a probability $0.5 \exp(-E/kT)$ at the site with the largest z coordinate. In real microemulsions neutral particles do occur, but in the model they are not allowed. As a consequence of this simplification, the creation and annihilation of charges cannot occur.

The charge exchange mechanism causes polarization of the clusters. When $N \gg 1$ it results in a huge increase of the electric current at percolation. As in conductivity experiments, the point where the electrical current increases suddenly is taken to be the percolation treshold. The increase of the current is expected at the moment that a cluster appears spanning the system in the z direction. Since charge hopping is allowed to 18 neighboring sites, the connectivity of a cluster is defined on the basis of the same coordination number of 18. Our use of different time scales for the particle motion and for the charge exchange leads to a dramatic increase of the numerical effort needed to simulate the model. Indeed, for $N = 1$, both mechanisms could be combined by allowing the exchange of particles together with the charge they carry. But at $N = 1$ there is not necessarily a huge increase of the electric current at percolation. Also, in the experimental system (water-in-oil microemulsions) charge exchange between neighboring droplets is much faster than the diffusion of individual droplets.

3. SIMULATIONS

We simulate a simple cubic lattice with size $W \times W \times L$ and periodic boundary conditions in all directions. In most of our simulations the system length L is 20 and the width W is 15.

The site percolation threshold for configurations with coordination number 18 is 13.7% (see ref. 38, Table I). The simulations reported below are executed for three different particle densities near the percolation treshold: $\rho = 0.08$, $\rho = 0.12$, and $\rho = 0.16$.

For simplicity we take $4J = 1$ everywhere. Since the effect of the electric field on the cluster shapes is most obvious below phase separation, almost all simulations are carried out in the latter region. Without an electric field, percolation is not possible for $\rho = 0.08$. Hence, in the simulations this density is studied most extensively because if percolation occurs, it can only be due to the electric field.

The simulations are implemented as quenches from high to low tem-

perature. In the starting configuration the particles are distributed randomly on the lattice. In principle it might be better to thermalize first before switching on the external electric field. In order to save computer time the quenching procedure was chosen.

Most simulations use $N=50$. However, at low temperatures percolation can be easily detected at lower N ($N=20$ or $N=10$), decreasing the amount of computer time. We checked that the change in N does not influence the cluster shapes or the configurations.

The measured quantities are the electric current i, the probabilities n_x and n_z that a particle has a neighbor in the x or the z direction, respectively, and the anisotropy of the clusters. They are measured as a function of time, but averaged over at least 1000 MCS.

For the current i, we subtract the number of charges moving against the field from those going with the field during one MCS. This quantity divided by the number of lattice sites is defined as the current i.

The probabilities n_x and n_z provide a simple way to determine the phase of the system. Indeed, in the condensed phase of the lattice gas both are high, since all particles are contained in one or a few compact clusters. In the gas phase both n_x and n_z have a low value. In addition, for $n_x \simeq n_z$ the clusters are nearly isotropic, while for $n_z \gg n_x$ they are elongated in the z direction.

An alternative quantity to measure the anisotropy of two-dimensional $L \times L$ systems with density $\rho=0.5$ has been introduced in ref. 6. A generalization to arbitrary density is

$$m=\frac{1}{\rho(1-\rho)}(\langle M_x^2\rangle-\langle M_y^2\rangle) \tag{3}$$

with

$$M_x^2=\frac{1}{L}\sum_y\left(\frac{1}{L}\sum_x t_{x,y}-\rho\right)^2 \tag{4}$$

and

$$M_y^2=\frac{1}{L}\sum_x\left(\frac{1}{L}\sum_y t_{x,y}-\rho\right)^2 \tag{5}$$

The quantities M_x^2 and M_y^2 measure the inhomogeneity of the system by calculating the mean square deviation from uniform density when projected on the y, resp. x coordinate axes. The definitions (4) and (5) deviate by a constant from those of ref. 7. In definition (3) the square root has been omitted because $\langle M_x^2\rangle-\langle M_y^2\rangle$ can be positive or negative. The

generalization to three-dimensional systems can be done in several ways. Because we consider a system size $W \times W \times L$ and expect clusters elongated along the z axis, the obvious definition is

$$m' = \frac{1}{\rho(1-\rho)} [\langle M_z^2 \rangle - 0.5(\langle M_x^2 \rangle + \langle M_y^2 \rangle)] \tag{6}$$

where

$$M_x^2 = \frac{1}{WL} \sum_{y,z} \left(\frac{1}{W} \sum_x t_{x,y,z} - \rho \right)^2 \tag{7}$$

$$M_y^2 = \frac{1}{WL} \sum_{x,z} \left(\frac{1}{W} \sum_y t_{x,y,z} - \rho \right)^2 \tag{8}$$

$$M_z^2 = \frac{1}{W^2} \sum_{x,y} \left(\frac{1}{L} \sum_z t_{x,y,z} - \rho \right)^2 \tag{9}$$

Clearly, the averages $\langle M_\alpha^2 \rangle$ (where $\alpha = x, y, z$) are zero, in the thermodynamic limit, for an isotropic homogeneous system. The combination $M_z^2 - 0.5(M_x^2 + M_y^2)$ should be zero for an isotropic cluster. However, this is only the case if $L = W$. Hence m' is a good measure for the anisotropy of the condensed phase provided the system is cubic ($L = W$) or for a nearly homogeneous system.

Marro *et al.*[4] introduced a slightly different definition:

$$m'' = \frac{1}{2[\rho(1-\rho)]^{1/2}} (M_v^2 - M_h^2)^{1/2} \tag{10}$$

with

$$M_v^2 = \frac{1}{W^2} \sum_{x,y} \left(\frac{2}{L} \sum_z t_{x,y,z} - 1 \right)^2 \tag{11}$$

and

$$M_h^2 = \frac{1}{L} \sum_z \left(\frac{2}{W^2} \sum_{x,y} t_{x,y,z} - 1 \right)^2 \tag{12}$$

Although the quantity m'' increases when a cluster elongates in the z direction, it does not really measure anisotropy. Indeed, from the inequality

$$M_v^2 = \frac{1}{W^2} \sum_{x,y} \left(\frac{2}{L} \sum_z t_{x,y,z} - 1 \right)^2$$

$$\geqslant \frac{1}{W} \sum_x \left(\frac{2}{LW} \sum_{y,z} t_{x,y,z} - 1 \right)^2 \tag{13}$$

it follows that for $L = W$ and a cubic invariant configuration one has $M_v^2 \geqslant M_h^2$. The equality holds only if the density is zero or one. Hence m'' is strictly positive for isotropic clusters, even when $L = W$.

4. SIMULATION RESULTS

4.1. Cluster Configurations and Time Evolution

At high temperatures the system is in the gas phase for all values of the electric field. Below some (field and density dependent) transition temperature three types of stationary states occur. At zero or low field the clusters are compact and nearly isotropic, as shown in Fig. 1a. Increasing the field causes elongation of the clusters. Above a field $E_1(\rho, T)$ this leads to a percolating cluster spanning the system between the two poles (Fig. 1b). Finally, for fields larger than some field $E_2(\rho, T)$ our simulations show a particle distribution like that in Fig. 1c. The configuration is about isotropic and similar to the configurations above the transition temperature at zero field.

The time evolution leading to configurations such as those in Figs. 1a and 1b is shown in Fig. 2 for three different field strengths at about the same temperature. Right after the quench the system condenses and approximately isotropic clusters are formed. For strong fields these clusters elongate immediately. As the electric field decreases, the elongation process takes more time. Near $E_1(\rho, T)$ one has to wait a long time before n_z, n_x, m', and m'' reach a final value. Note that the evolution of the system toward the stationary state is rather continuous.

For fields slightly smaller than $E_2(\rho, T)$ one observes an interesting effect. There is an immediate but small elongation. Some time later the parameters n_z, n_x, m', and m'' suddenly change and percolation sets in (see Fig. 3). A delayed abrupt change of the parameter m'' occurs for similar densities and strong fields $E \to \infty$ in the two-dimensional driven lattice gas (see Fig. 3 in ref. 7). In the polarized lattice gas, the discontinuous behavior is observed only for fields lying in a narrow interval just below $E_2(\rho, T)$.

We checked that after turning off the field a percolating cluster as in Fig. 1b disappears and the system becomes isotropic again (see Fig. 4). The figure illustrates also that for lower temperatures it takes longer to reach a stationary state. As an alternative one might replace the thermal quench procedure by the heating of a single-component strip containing all the particles.[6,7] We have not performed such simulations.

The time evolution of the electric current is shown in Fig. 5 for the same parameters as in Fig. 2. From comparison with Fig. 2, it is obvious that the electric current and the elongation are closely related. For suf-

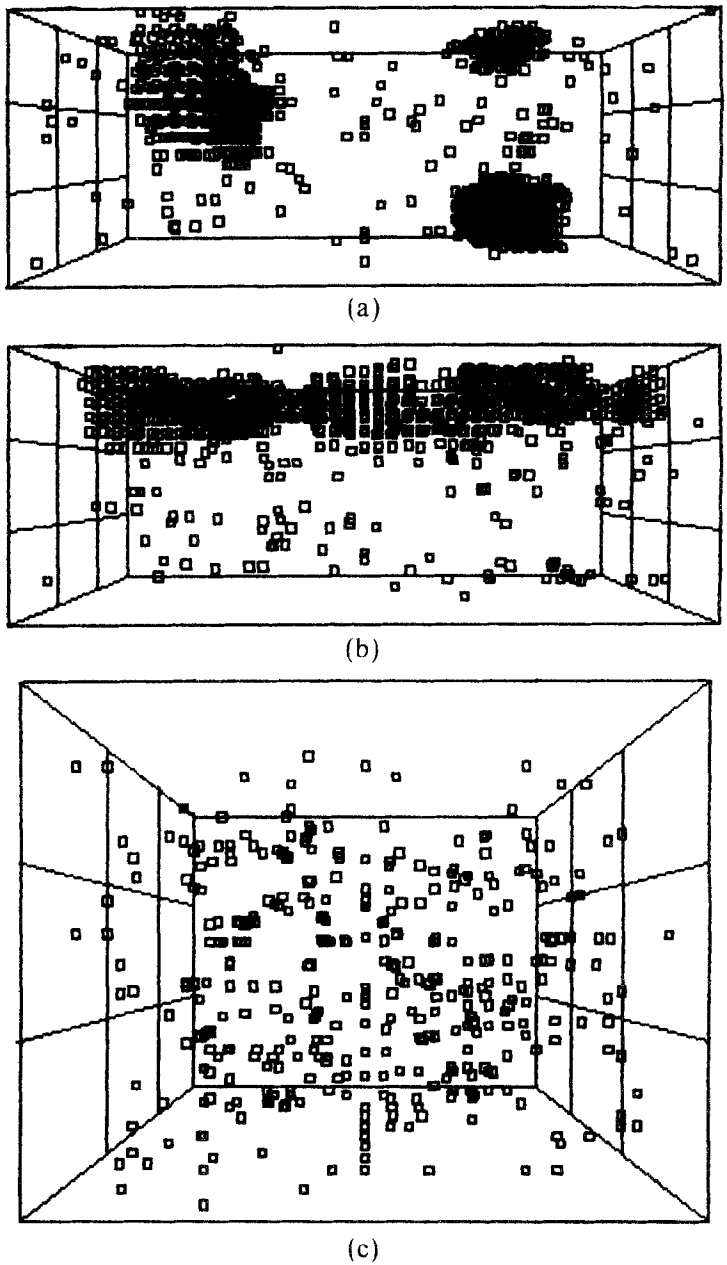

Fig. 1. Three-dimensional view of a particle configuration. (a) At $E = 0$, $kT = 0.60$, $\rho = 0.08$, $t = 20000$ MCS, in a $15 \times 15 \times 40$ system; (b) at $E = 0.15$, $kT = 0.60$, $\rho = 0.08$, $t = 20000$ MCS, in a $15 \times 15 \times 40$ system; (c) at $E = 0.90$, $kT = 0.60$, $\rho = 0.08$, $t = 18000$ MCS, in a $15 \times 15 \times 20$ system.

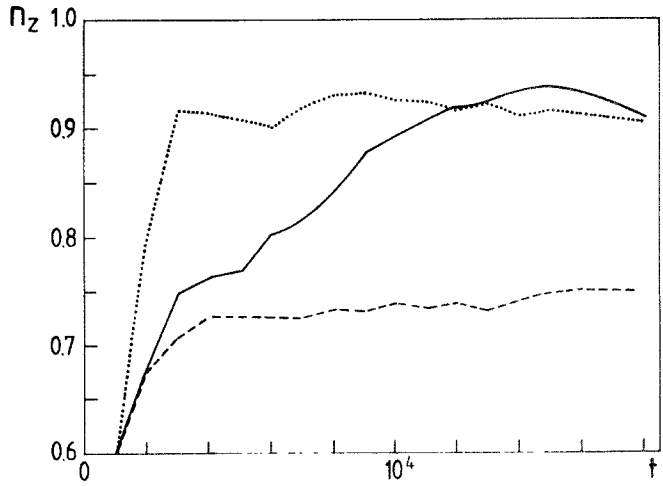

Fig. 2. Probability n_z that a particle has a neighbor in the positive z direction. The simulations are done on a $15 \times 15 \times 20$ system with $\rho = 0.08$ and different values of the temperature and the electric field: $kT = 0.45$ and $E = 0.025$ (– –), $kT = 0.40$ and $E = 0.125$ (·), and $kT = 0.40$ and $E = 0.40$ (···). The curves for n_x and n_y coincide within error flags with the dashed line.

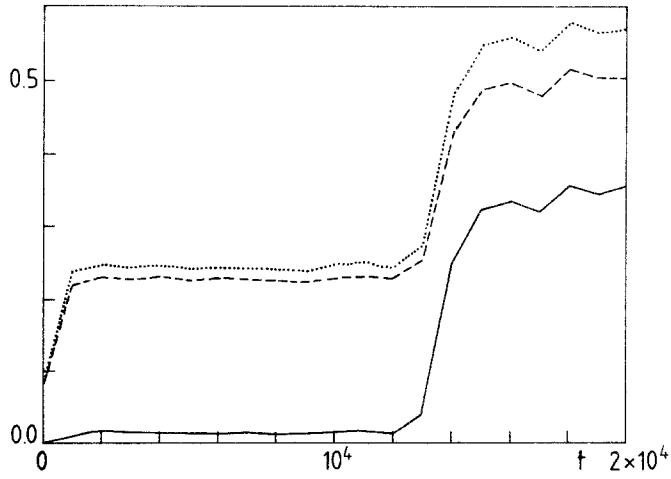

Fig. 3. Probabilities n_z (···) and n_x (– –) as a function of time for $\rho = 0.08$, $E = 0.60$, and $kT = 0.65$. (—) is the function m''.

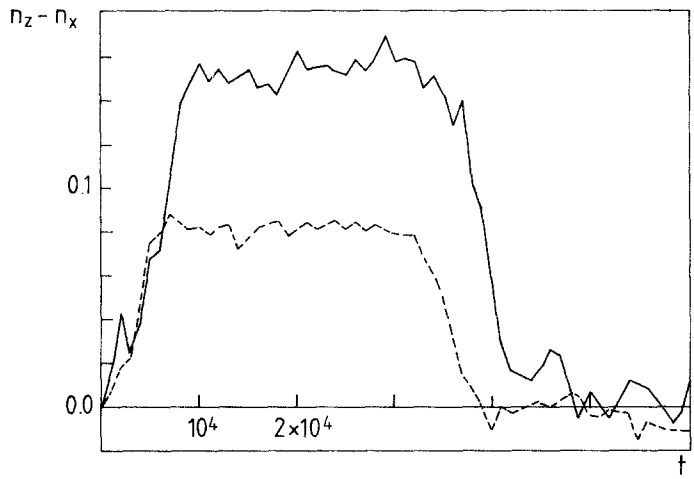

Fig. 4. Anisotropy $n_z - n_x$ versus time on a $15\times15\times20$ system with the field turned on at $t=0$ and switched off at $t=3\times10^4$ MCS; the parameters are $\rho=0.12$, $kT=0.65$, $E=0.15$ (- -) and $\rho=0.08$, $kT=0.50$, $E=0.15$ (—). Note that for the lowest temperature ($kT=0.50$) the anisotropy is largest. For $kT=0.5$ it takes also more time to reach the stationary state.

ficiently strong fields, fast charge exchange in percolating clusters leads to a huge current. For low fields the current is only due to the diffusion of very few isolated particles and thus is small. For low temperatures we never saw a percolating cluster split and disappear. For higher temperatures, near $E_1(\rho, T)$, the percolating cluster can be destroyed temporarily by thermal motion. Then the current shows an intermittent behavior as in Fig. 6.

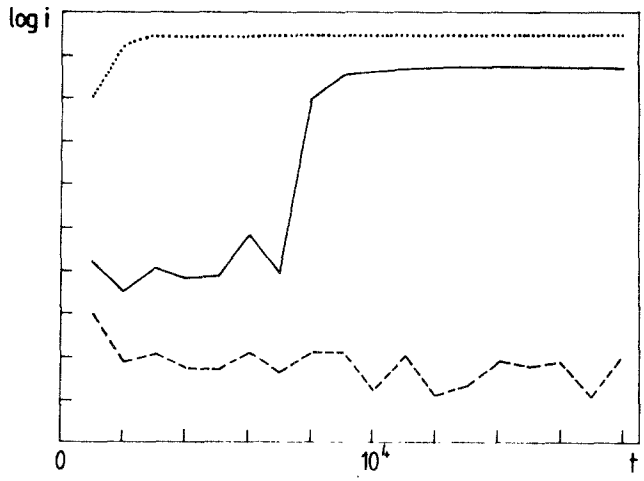

Fig. 5. Electric current versus time. The lines are as in Fig. 2.

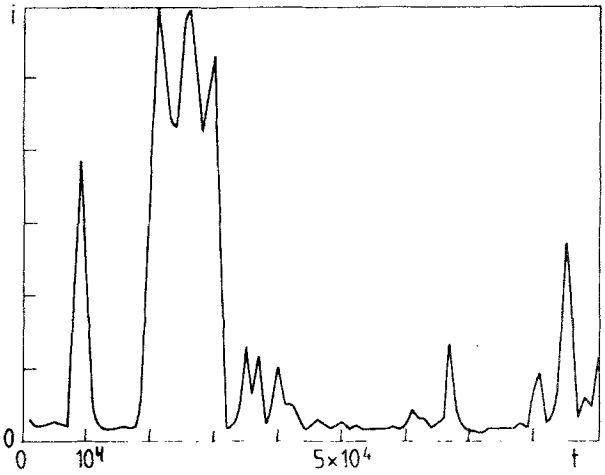

Fig. 6. Current versus time at $\rho = 0.08$, $kT = 0.65$, and $E = 0.11$ in a $15 \times 15 \times 20$ system.

4.2. Comparison with the Driven Lattice Gas Model

At density $\rho = 0.5$ and at low temperature the two- and three-dimensional driven lattice gas models remain anisotropic for $E \to \infty$.[4,6] This result is also found[7] in two dimensions for densities smaller than 0.5. Clearly, the behavior differs from that of the present model, which shows a gas phase in the presence of strong fields. For a better understanding of these differences we have studied also a version of the driven lattice gas model where, as in our model, the particles can jump to 18 neighboring sites instead of the usual six. We refer to the latter model as DLG18. It reduces to the usual driven lattice gas model (DLG6) when jumps are allowed to nearest neighbors only. For $\rho = 0.08$, $kT = 0.65$, and $E \to \infty$ both the polarized lattice gas and DLG18 have a gas phase as in Fig. 1c. The fact that allowing jumps to 6 instead of 18 neighboring sites leads to a completely different stationary state suggests that steric hindrance effects are essential in the formation of the strip phase. The obvious explanation is the following. At large E the motion of a particle along the direction of the field is not hindered by the attraction of other particles. Indeed, the electric potential always dominates the attraction forces. For a coordination number six, the only site in the direction of the field is occupied with high probability. The situation changes if a particle is allowed to jump to next nearest neighbors as well. Then it has five sites instead of one to which it can jump driven by the field. In addition, the transverse component of the jump vector along diagonal directions (x–z and y–z) experiences a random driving field, which means that there is an increase of the effective

temperature in the direction orthogonal to the field. Thus, ordering is impossible and a gas phase results. For the sake of completeness we mention that both the polarized lattice gas with coordination number 18 and that with coordination number 6 have always a gas phase for $E \to \infty$. This is explained by a reduced importance of the steric hindrance, since in the polarized lattice gas only half of the particles try to move in the direction of the field (the other half move in the opposite direction). One concludes that steric hindrance is the dominant effect in DLG6 and that its reduction by an increased effective temperature leads to the gas phase of DLG18 at $E \to \infty$.

We compared also the cluster configurations of the polarized lattice gas, of model DLG6, and of model DLG18 at $\rho = 0.08$, $kT = 0.65$, and for different values for the electric field E. It appears that at field strengths for which the polarized lattice gas already percolates, DLG6 and DLG18 are still nearly isotropic. The explanation is that the electrostatic forces on both ends of a polarized cluster are opposite and try to separate both ends from each other, which results in an elongation of the cluster. In DLG6 and DLG18 the electrostatic force on every particle has the same direction and the elongation remains modest. Polarization, caused by the introduction of two opposite charges, is in fact a major difference between the driven and the polarized lattice gas.

4.3. Electric Field Dependence

The stationary values of the anisotropy parameters as a function of the electric field for $\rho = 0.08$ and $kT = 0.65$ are shown in Fig. 7. For the same parameters, the conductivities as a function of small fields are shown in Fig. 8, the electric currents in Fig. 9. From these figures one notes that for small fields the clusters are nearly isotropic ($n_y \simeq n_z$). There is no percolation. At high field strength, the clusters elongate and the anisotropy of the system increases. Between $E_1 \simeq 0.1$ and $E \simeq 0.15$ the current is intermittent. In this region the part of the time the system percolates increases with the field. For fields larger than $\simeq 0.15$ but smaller than $\simeq 0.62$ the system percolates permanently. Apart from the intermittent region, Ohm's law is fulfilled for $E/kT \ll 1$ (see Fig. 7). For larger fields, the relation between current and field becomes highly nonlinear. If the electric field is larger than $E_2 \simeq 0.62$, a gas phase is formed. In the gas, the clusters remain slightly elongated ($n_z > n_x$). For the behavior of the parameter m'' around $E = 0$, we refer to the discussion in Section 3. Note also that a change of the width of the system causes a shift of the fields E_1 and E_2. The size dependence of the simulations is discussed in Section 5.

We now discuss the decrease of the anisotropy with increasing field in

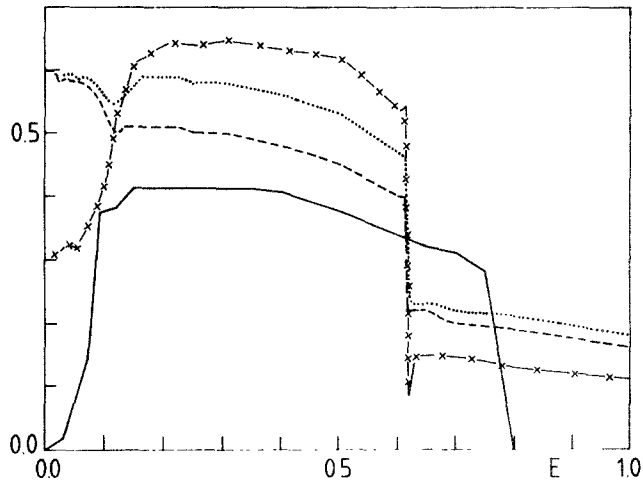

Fig. 7. Cluster anisotropy as a function of electric field for $\rho = 0.08$ and $kT = 0.65$ on a $15 \times 15 \times 20$ system: n_z (···), n_x (- -), and m'' (·). ( ) is the anisotropy m for $\rho = 0.08$ and $kT = 0.65$ on a $20 \times 20 \times 20$ system. Note that the change of the width W of the system causes a shift of E_1 and E_2.

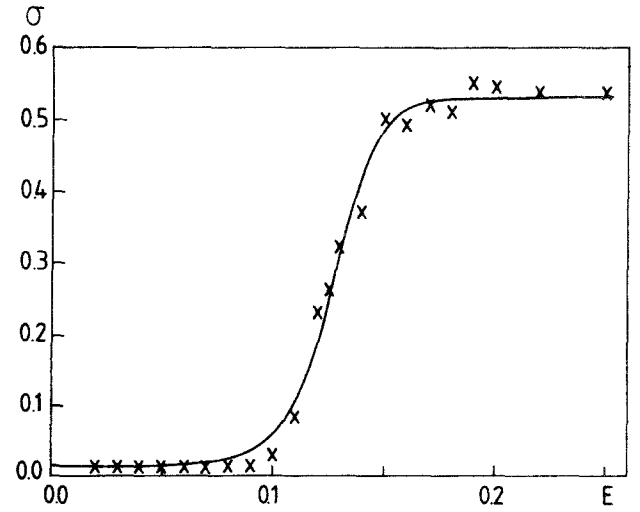

Fig. 8. Conductivity versus field at $kT = 0.65$. The crosses are the measured points, after averaging. The dotted curve is the result of a fit with the formula $\sigma = \sigma_0 + \sigma_1 \tanh c(E^2 - E_0^2)$, where σ_0, σ_1, E_0^2, and c are fit parameters.

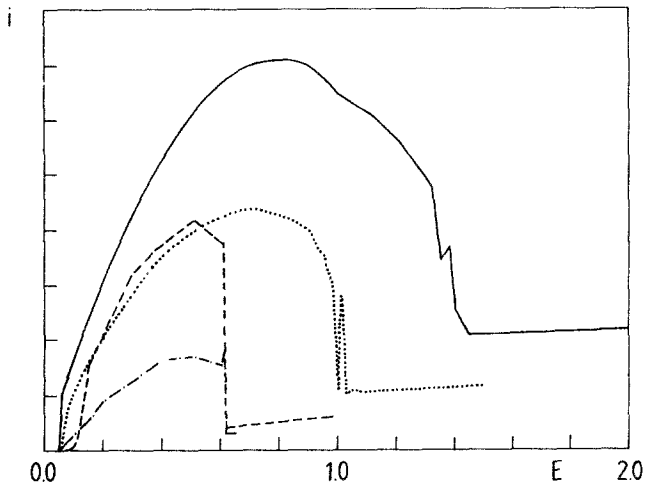

Fig. 9. Electric current as a function of the field E on a $15 \times 15 \times 20$ system for $kT = 0.65$ and density $\rho = 0.08$, $\rho = 0.12$ ($\cdots$), and $\rho = 0.16$ (—). For density $\rho = 0.08$ the current is shown for $N = 50$ (– –) and $N = 20$ (– –). For $\rho = 0.12$ and $\rho = 0.16$ we took $N = 20$.

the percolating regime $E_1 < E < E_2$. The same effect has been observed in the driven lattice gas (see Fig. 10 of ref. 2) and the tentative explanation given there holds here, too. The electric field induces two opposing effects: (1) at low field strength there is a competition between the surface energy and the electric field potential, leading to elongation of the clusters; (2) once a percolating cluster is formed, the polarization disappears and the correlations along the field direction decrease. In addition, the strong electric field facilitates the escape of particles from the cluster, which has the same effect as increasing the temperature. This is confirmed by a decrease of the number of particles in the percolating cluster. See Fig. 10, showing a configuration for an electric field E slightly below E_2 ($E_2 \simeq 0.75$). Note the increased amount of isolated particles compared to Fig. 1b.

The electric current as a function of the electric field shows the same three regimes (see Fig. 9). Recall that N is the number of times that the charge exchange algorithm is executed after each completion of the particle–hole exchange algorithm. By changing N, we can deduce the nature of the electric current. For one density Fig. 9 shows the electric current for two different values of N: $N = 20$ and $N = 50$. One sees clearly that the transition fields E_1 and E_2 do not depend on N. Below E_1 the electric current is independent of N. This confirms that the current is carried by diffusing particles. For fields $E > E_1$ and for which Ohm's law is valid, the current is proportional to N. This indicates it is mainly due to charge exchange. Note that the current decreases in the same region below E_2,

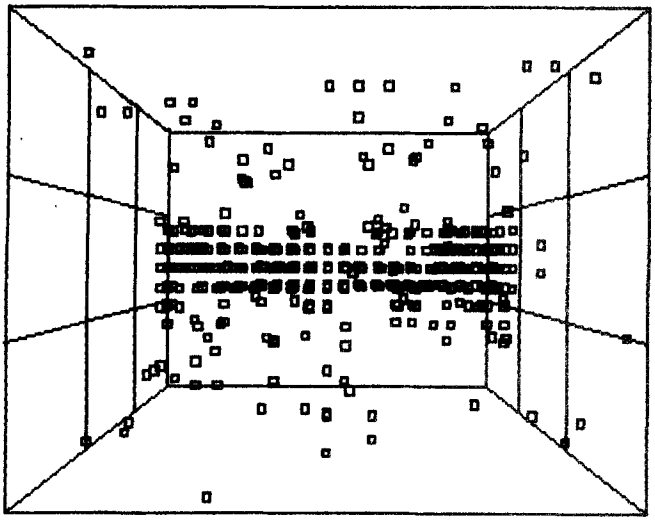

Fig. 10. Three-dimensional view of the particle configuration at $\rho = 0.08$, $E = 0.60$, $kT = 0.60$, $t = 20000$ MCS on a $15 \times 15 \times 20$ lattice.

where also the anisotropy decreases. The explanation is again the lower number of particles in the percolating cluster. In the gas phase $E > E_2$ the current is mainly but not exclusively due to particle diffusion.

We checked that at density $\rho = 0.16$ and in the gas phase ($E > E_2$) there is most of the time a percolating cluster (with respect to coordination number 18). However, this cluster is ramified and of a dynamic nature. This explains why the current is smaller than in the $E < E_2$ regime, but significantly larger than for $E > E_2$ at densities $\rho = 0.08$ and $\rho = 0.12$. Ramification of the percolating cluster reduces charge exchange in two ways: (i) the average number of neighbors decreases; the latter reduces the number of sites to which hopping is possible; (ii) at large fields, charges are trapped in dangling ends (see, e.g., ref. 37 and references quoted there).

4.4. Phase Diagram

The most important result of our simulations is the phase diagram of Fig. 11. Three stationary phases are found: (1) a gas phase for high temperature or high field; (2) an approximately isotropic two-phase region for low fields and intermediate temperature; (3) an anisotropic two-phase striplike region with a cylinder-shaped percolating cluster for intermediate field and temperature. In addition, we observe a region of intermittency at the higher temperature side of phase (3). This region is rather small and is not shown in Fig. 11. The separation line between the gas phase (1) and the

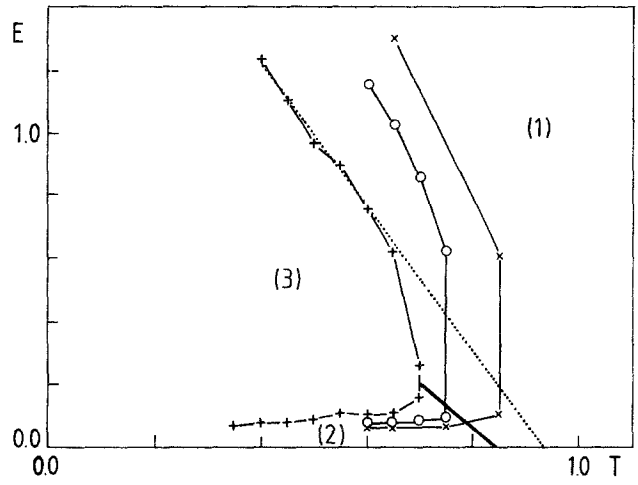

Fig. 11. Phase diagram for densities $\rho = 0.08$ (+), $\rho = 0.12$ (○), and $\rho = 0.16$ (*) on a $15 \times 15 \times 20$ system. The boundary between phases (1) and (2) has not been calculated, but for reasons of clarity it is drawn at its estimated position. The dotted line is fitted according to formula (14).

isotropic region (2) has not been determined. It has been drawn in Fig. 11 at the place where we suspect it to be. The fields $E_1(\rho, T)$ and $E_2(\rho, T)$ give the boundaries between phases (2) and (3), and between phases (1) and (3), respectively. We introduce the temperature $T^*(\rho)$ by the condition $E_1(\rho, T^*) = E_2(\rho, T^*)$. Its value as a function of density is found to be

$$T^*(\rho = 0.08) = 0.72 \pm 0.02 \qquad T_c(\rho = 0.08) = 0.93$$
$$T^*(\rho = 0.12) = 0.81 \pm 0.03 \qquad T_c(\rho = 0.12) = 1.00$$
$$T^*(\rho = 0.16) = 0.87 \pm 0.02 \qquad T_c(\rho = 0.16) = 1.04$$

For comparison we show also the phase separation temperature without electric field $T_c(\rho)$ as calculated using the Padé approximation results by Essam and Fisher[36] and the value $kT_c \simeq 1.12$ at density $\rho = 0.5$ (see ref. 35). The transition temperatures as found in the simulations at $E = 0$ are considerably lower.[39] The effect is due to the fact that the simulations are done with a constant number of particles and not at constant pressure. However, the temperature $T^*(\rho)$ is still lower than the one observed by simulation in the absence of electric field. Finally, it is clear that the temperature $T^*(\rho)$ is sensitive to finite-size effects.

Apparently, the electric field E_2 is linear in the temperature T, at least

for low temperatures. This can be understood by the following reasoning. At low temperature the probability that a particle leaves a cluster is very small except when it moves in the direction of the field. Let Δn denote the decrease in the number of nearest neighbors when the particle leaves the cluster. Then the change in energy is $4J\Delta n - E$. The probability to leave a cluster is roughly proportional to $\exp[-(4J\Delta n - E)/k_B T]$ and can be assumed in first instance to be constant along the line $E_2(\rho, T)$. Hence one obtains

$$E_2(\rho, T) = 4J\Delta n - cT \tag{14}$$

where c is a constant. For sufficiently low temperature Δn is independent of temperature. Hence a linear behavior is obtained (see Fig. 11). For $\rho = 0.08$ the fit gives $\Delta n = 2.3 \pm 0.2$.

The increase of $E_1(\rho, T)$ with temperature is in agreement with the observed decrease of anisotropy with temperature (see Fig. 12). It is a consequence of the competition between temperature and electric field. One sees also from Fig. 12 that m'' changes continuously between low- and high-temperature phases due to the intermittent behavior in the vicinity of the $E_1(\rho, T)$ line. In the driven lattice gas, at densities $\rho < 0.2$ and $E \to \infty$, the parameter m'' jumps discontinuously when passing from phase (2) to phase (3). As expected, at constant field strength both n_z and n_x are

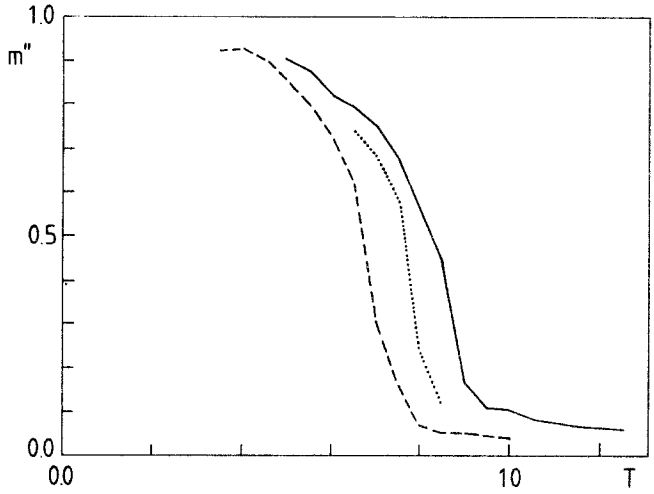

Fig. 12. Plot of m'' as a function of temperature at $E = 0.15$ for $\rho = 0.08$ (– –), $\rho = 0.12$ (· · ·), and $\rho = 0.16$ (—) on a $15 \times 15 \times 20$ lattice.

decreasing functions of temperature. Because of the increased anisotropy at lower temperatures, the difference $n_z - n_x$ increases also when lowering the temperature (see Fig. 4). For small electric fields $E < E_2(\rho, T)$ the behavior of n_z and n_x as a function of both temperature and electric field is similar to the two-dimensional driven lattice gas for $\rho = 0.5$ (see Fig. 10 of ref. 2).

4.5. Temperature Dependence of the Electric Current

Figure 13 shows the conductivity in the limit of zero field $E = 0$. Above the phase separation temperature $T_c(\rho)$ the conductivity is nearly constant and the Ohmic region extends to large E values. At low temperatures most of the particles condense and the conductivity drops to almost zero.

The behavior of the conductivity versus field at different temperatures is shown in Fig. 14. For the highest temperature shown the strip phase is not entered and the conductivity is nearly constant. At lower temperatures one notes a huge increase of the current when passing through the strip phase. Note also that at sufficiently low temperatures intermittency disappears and the current is discontinuous near $E_1(\rho, T)$.

Finally, Figure 15 shows the conductivity as a function of temperature at constant field $E = 0.15$. For the same parameters, the quantity m'' is shown in Fig. 12. For $\rho = 0.16$ the current starts to increase when the

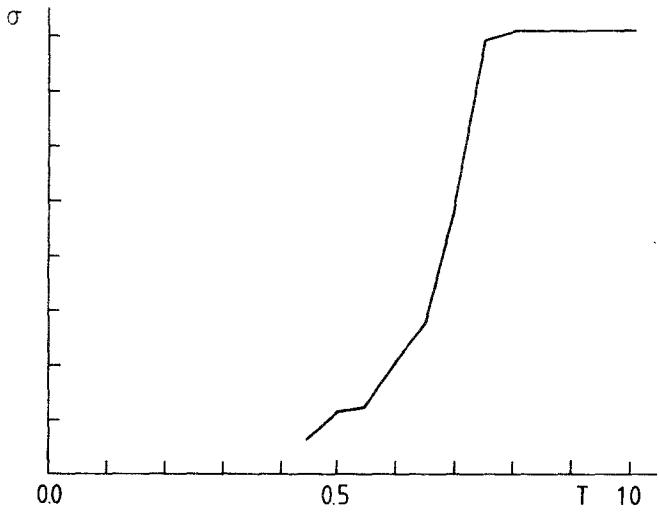

Fig. 13. Conductivity as a function of temperature on a $15 \times 15 \times 20$ lattice with density $\rho = 0.08$.

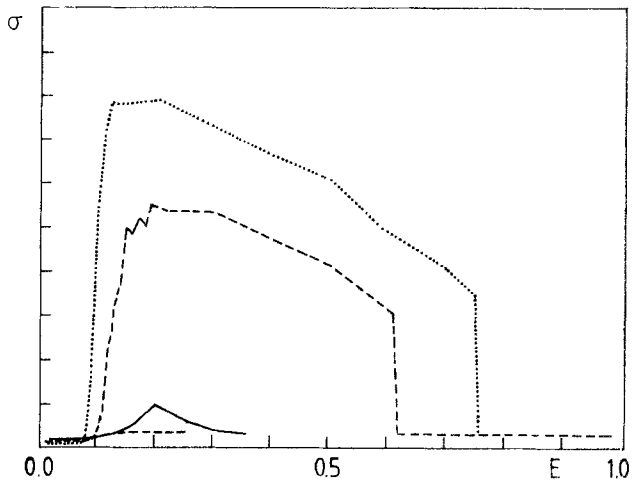

Fig. 14. Conductivity versus electric field at $\rho = 0.08$ on a $15 \times 15 \times 20$ lattice for different temperatures: $kT = 0.60$ (···), $kT = 0.65$ (– – –), $kT = 0.70$ (·), and $kT = 0.75$ ( ).

percolating cluster changes from ramified to compact. For $\rho = 0.08$ the increase occurs at the moment that the percolating cluster appears. Note also that below phase separation the conductivity is approximately a linear function of temperature. One should not compare the slopes of both curves, since the simulations were done with $N = 50$ for $\rho = 0.08$ and $N = 20$ for $\rho = 0.16$.

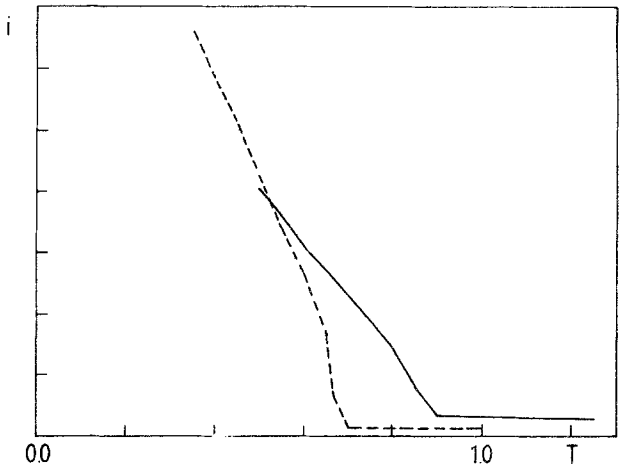

Fig. 15. Electric current as a function of temperature on a $15 \times 15 \times 20$ lattice for $E = 0.15$ and densities $\rho = 0.08$ (– –) and $\rho = 0.16$ (—).

5. CONCLUSIONS

The present paper introduces a lattice gas model in which the particles have charge either $+1$ or -1. Accordingly, they drift in opposite directions under the influence of an external electric field. In this aspect the model differs from the driven lattice gas, where all particles move in the same direction. In the present model charge separation occurs and leads to elongation of clusters of particles even at rather small values of the electric field. In the driven lattice gas one observes a dynamic transition to a striplike configuration of high- and low-density regions. A similar transition occurs in the present model for much lower values of the electric field precisely because of the elongation of the clusters facilitating the transition.

A new feature of the present study is the use of a high coordination number (18) for the dynamics of particles and charges. Steric hindrance plays an important role in the driven lattice gas with coordination number 6 and stabilizes the striplike configuration at large electric fields. With the coordination number of 18 the system stays in the gas phase for large electric fields down to low temperatures. For the present model the gas phase is observed at high fields, even with coordination number 6.

A difficult aspect of the present study concerns the finite-size effects. We have simulated only the three-dimensional model. The system sizes are rather small ($15 \times 15 \times 20$ up to $20 \times 20 \times 60$). Finite-size effects are in any case important, especially because the electric field leads to long-range correlations in the z direction. Indeed, percolation is reached as soon as the length of an elongated cluster equals the size of the system. In addition, because of periodic boundary conditions both ends of the elongated cluster touch each other at percolation. Finally, due to the small system size, only one percolating cluster is present. In a large system we expect that in the strip phase several percolating clusters span the system in the z direction. Such finite-size effects are of a quantitative nature and we do not expect any qualitative change of the phase diagram of Fig. 11. We checked that simulations for different system sizes ($15 \times 15 \times 20$, $15 \times 15 \times 40$, and $20 \times 20 \times 60$ at $kT = 0.60$, $E = 0.15$, and $\rho = 0.08$) in all cases produce a similar stationary configuration (see Fig. 1b) with an elongated cluster spanning the system in the z direction.

REFERENCES

1. S. Katz, J. L. Lebowitz, and H. Spohn, *Phys. Rev. B* **28**:1655 (1983).
2. S. Katz, J. L. Lebowitz, and H. Spohn, *J. Stat. Phys.* **34**:497 (1984).
3. H. van Beijeren, R. Kutner, and H. Spohn, *Phys. Rev. Lett.* **54**:2026 (1985).
4. J. Marro, J. L. Lebowitz, H. Spohn, and M. Kalos, *J. Stat. Phys.* **38**:725 (1985).
5. J. Vallés and J. Marro, *J. Stat. Phys.* **43**:441 (1986).

6. J. Vallés and J. Marro, *J. Stat. Phys.* **49**:89 (1987); **51**:321 (1988).
7. J. Marro and J. Vallés, *J. Stat. Phys.* **49**:121 (1987).
8. J. Marro, in *Fluctuations and Stochastic Phenomena in Condensed Matter* (Lecture Notes in Physics 268), L. Garrido, ed. (Springer-Verlag, Berlin, 1987), p. 227.
9. H. Spohn, *Ann. N. Y. Acad. Sci.* **491**:157 (1987).
10. M. Q. Zhang, J.-S. Wang, J. L. Lebowitz, and J. L. Vallés, *J. Stat. Phys.* **52**:1481 (1988).
11. K.-t. Leung, K. K. Mon, J. L. Vallés, and R. K. P. Zia, *Phys. Rev. Lett.* **61**:1744 (1988).
12. K.-t. Leung, B. Schmittmann, and R. K. P. Zia, *Phys. Rev. Lett.* **62**:1772 (1989).
13. J. L. Vallés, K.-t. Leung, and R. K. P. Zia, *J. Stat. Phys.* **56**:43 (1989).
14. H. van Beijeren and L. S. Schulman, *Phys. Rev. Lett.* **53**:806 (1984).
15. J. Krug, J. L. Lebowitz, H. Spohn, and M. Q. Zhang, *J. Stat. Phys.* **44**:535 (1986).
16. A. Coniglio, C. Nappi, F. Peruggi, and L. Russo, *J. Phys. A* **10**:205 (1977).
17. H. Müller-Krumbhaar, *Phys. Lett.* **50A**:27 (1974).
18. D. Heermann and D. Stauffer, *Z. Phys. B* **44**:339 (1981).
19. M. Lagues, *J. Phys.* (Paris) **40**:L331 (1979).
20. A. M. Cazabat, D. Chatenay, D. Langevin, and J. Meunier, *Faraday Disc. Chem. Soc.* **76**:291 (1982).
21. H.-F. Eicke, R. Hilfiker, and M. Holz, *Helv. Chim. Acta* **67**:361 (1984).
22. M. A. Van Dijk, *Phys. Rev. Lett.* **55**:1003 (1985).
23. S. Battacharya, J. Stokes, M. W. Kim, and J. S. Huang, *Phys. Rev. Lett.* **55**:1884 (1985).
24. H.-F. Eicke, R. Hilfiker, and H. Thomas, *Chem. Phys. Lett.* **125**:295 (1986).
25. S. Safran, I. Webman, and G. Grest, *Phys. Rev. A* **32**:506 (1985).
26. A. Bug, S. Safran, and G. Grest, *Phys. Rev. Lett.* **55**:1896 (1985).
27. N. Seaton and E. Glandt, *J. Chem. Phys.* **86**:4668 (1987); **87**:1785 (1987).
28. G. S. Grest, I. Webman, S. A. Safran, and A. L. R. Bug, *Phys. Rev. A* **33**:2842 (1986).
29. S. Geiger, H.-F. Eicke, and D. Spielmann, *Z. Phys. B* **68**:175 (1987).
30. G. E. Pike and C. H. Seager, *Phys. Rev. B* **10**:1421 (1974).
31. H.-F. Eicke, R. Hilfiker, and H. Thomas, *Chem. Phys. Lett.* **120**:272 (1985).
32. H.-F. Eicke and J. Naudts, *Chem. Phys. Lett.* **142**:106 (1987).
33. M. Aertsens and J. Naudts, in *Phase Transitions in Soft Condensed Matter*, T. Riste and D. Sherrington, eds. (Plenum Press, New York, 1989), p. 203.
34. H.-F. Eicke, M. Borkovec, and B. Das-Gupta, *J. Phys. Chem.* **93**:314 (1989); M. Paillette, Private communication.
35. C. Domb, in *Phase Transitions and Critical Phenomena*, Vol. 3, C. Domb and M. S. Green, eds. (Academic Press, London, 1974), p. 357.
36. J. Essam and M. Fisher, *J. Chem. Phys.* **38**:802 (1963).
37. R. B. Pandey, *Phys. Rev. B* **30**:489 (1984).
38. R. B. Stinchcombe, in *Phase Transitions and Critical Phenomena*, Vol. 7, C. Domb and J. L. Lebowitz, eds. (Academic Press, London, 1983), p. 151.
39. D. P. Landau, *Phys. Rev. B* **14**:255 (1976).